

A High Voltage Gain Boost Converter: Concept of DC Power Transfer Using Mutual Inductors

Saurav Bharadwaj¹, Indrajit Barman², Midar Riba³, Asish Arpan Dadhara⁴, Biswajit Sengupta⁵

^{1,2,3,4,5}Don Bosco College of Engineering and Technology, Assam Don Bosco University
Airport Road, Azara, Guwahati - 781017, Assam, INDIA.

¹sauravbharadwaj41@gmail.com*, ⁵biswajit.sengupta@dbuniversity.ac.in

Abstract: A high voltage boost converter is being prototyped in an artificial software based environment of MATLAB/ SIMULINK and identifies the practical conditions of the converter. A direct current (DC) input voltage is being boosted to a higher magnitude by multiplying a gain factor in a dynamic process of DC power transfer by cascading three mutual inductors in a single core. Input voltage is being switched by primary IGBT switches creating simultaneous charging and discharging of primary inductor, hence induces identical voltage in two secondary inductors. Inductors are charged and power is transferred to a parallel capacitor and finally to the resistive load in accurate control of duty cycles.

Keywords: Coupled inductors, Voltage spikes, Semi-conductor switches, Switching frequency, Voltage boosting, DC power transfer and Voltage ripples.

1. Introduction

Boost converters consist of an inductor switched by a semi-conductor switch in a periodic phenomenon of charge and discharge in transferring the power to a parallel resistance-capacitance pair, limiting the DC voltage transfer gain to 2-3 times of the input voltage. The applications of the boost converter are not only limited to power plants and grids but also in multi-disciplinary functional systems. In large applications of these converters, it is a challenge to design a modified converter providing all the necessary parameters. A number of designers and researchers use various techniques to boost the input voltage including parallel inductors to a capacitor, single inductor to parallel capacitors, concept of mutual inductors and transformers and some complex circuitry for efficient power transfer. An important parameter of any converter is its practical stability; designing in an artificial environment like Simulink limits its practical operational analysis. The disadvantage of the software is that it is unable to determine exact physical disturbances, noises and other factors effecting each modal operation. On the other hand, it is mandatory to design in such artificial environment initially considering the maximum possible practical cases. Finally, a general boost converter loses its boosted power in power switches, inductors and series circuits of resistors and capacitors.

In the paper, a high voltage boost converter is designed using the principle of DC power transfer using mutual inductors. Boost converter can produce a significant amount of voltage of higher

magnitude. A number of simulation issues and conditions of software failure can be defined from this innovative design in the artificial environment.

2. High Voltage Gain Boost Converter

High voltage gain boost converter circuit is designed for an input voltage of 100V, applied to the primary of the three mutual inductors (fig. 1). Each of the identical inductor has an inductance and a resistance of 50mH and 5Ω respectively. Coefficient of coupling is considered depending on how the coils are wound in the core and these coupled coils have a mutual inductance and resistance of 1μH and 1Ω respectively. Four switches are being configured in the model and are switched in independent periodic duties depending on the directional flow of current and flux. Mutual coupled inductors play an important role in inducing voltage due to dynamic change in current of the inductors and charge transfer to a parallel capacitor and resistive load.

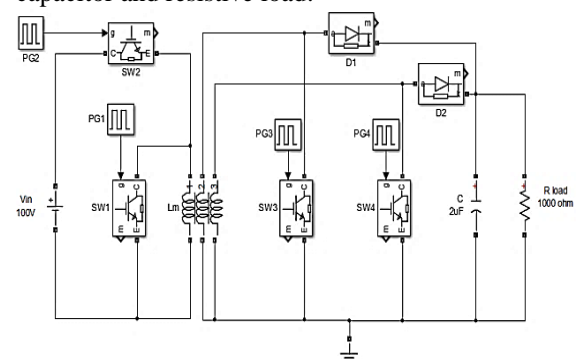


Figure1: High Voltage Gain Boost Converter

3. Operations and Modes

In modeling of the circuit (fig. 2, 3 and 4), four switches are switched in different time intervals.

Comparing the three switching intervals in a single time axis, switching periods of SW₁ and SW₂ is periodically repeated in switching curve of SW₃ and SW₄ (fig.2).



Figure 2: Time Intervals of Different Modes

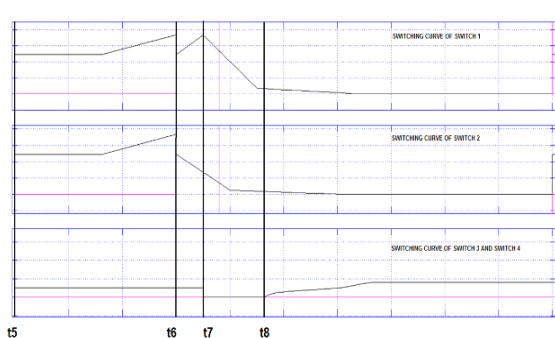
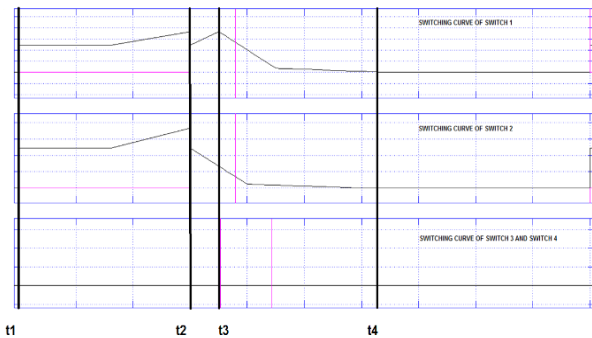


Figure3: Time Intervals of t₁ to t₄ Figure4: Time Intervals of t₅ to t₈

Mode 1 (t₁-t₂):

In this time interval, switches SW₁ and SW₂ are switched in a periodic interval causing a phenomenon of charging and discharging, where SW₁ has an initial delay of 50us. A charging current of i₁(t) and discharging current of i₂(t) of the primary inductor changes fluxes in the secondary inductors. Currents i₄(t) and i₅(t) induced in the secondary inductors L₂ and L₃ produces a voltage V₂(t) which charge the capacitor C with a current of i₆(t) and providing power to the load (fig.5).

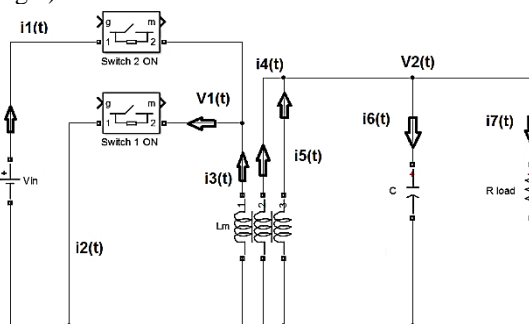


Figure 5: Mode 1 Operation

Mode 2 (t₂-t₃):

In this time interval, switches SW₁ is turned on and inductor L₁ finds a path to discharge. Secondary currents i₂(t) and i₃(t) induced in the inductors, L₂ and L₃ produce a nodal voltage V(t) and currents i₄(t) and i₅(t) flows through the capacitor to charge and the resistive load (R_{load}) respectively (fig. 6).

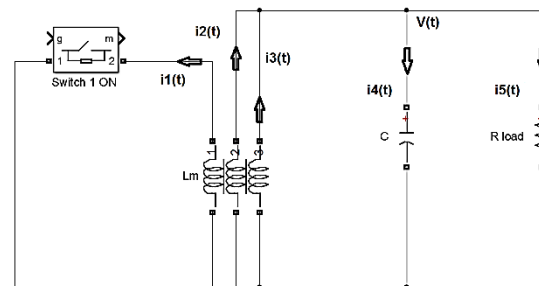


Figure 6: Mode 2 Operation

Mode 3 (t₃-t₄):

In this time interval, all the switches are turned off and the primary inductor is open circuited. Secondary currents, i₁(t) and i₂(t) passes through the

inductors, L_2 and L_3 results in charging of capacitor through current $i_3(t)$ and dissipates power in the load.

Since, time durations of all the switches are not identical, so time laps between duration of time t_4 and t_5 is omitted as a number of repeated time periods of SW_1 and SW_2 is present within a time period of SW_3 and SW_4 (fig. 7).

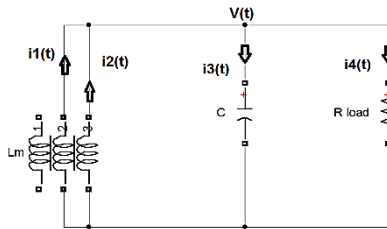


Figure 7: Mode 3 Operation

Mode 4 (t_5-t_6):

In this time interval, all the switches are turned on and secondary inductors L_2 and L_3 are being charged by the currents $i_4(t)$ and $i_5(t)$ as primary inductor current creates a flux due to the change in current $i_3(t)$. Simultaneously capacitor is responsible to maintain a constant output voltage and starts discharging in a condition as change in voltage drops across the load are negligible (fig. 8).

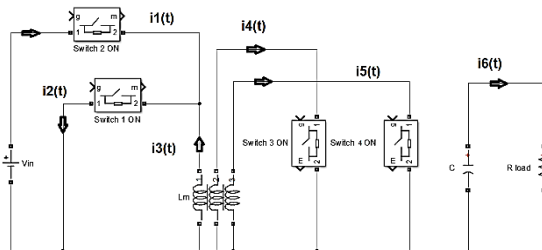


Figure 8: Mode 4 Operation

Mode 5 (t_6-t_7):

In this time interval, the primary inductor is responsible to charge the secondary inductors by induced current $i_2(t)$ and $i_3(t)$. Gradually, the current in the primary inductor and capacitor $i_1(t)$ and $i_4(t)$ respectively starts to decrease but before reaching a nominal lower value the circuit operates in the corresponding mode (fig. 9).

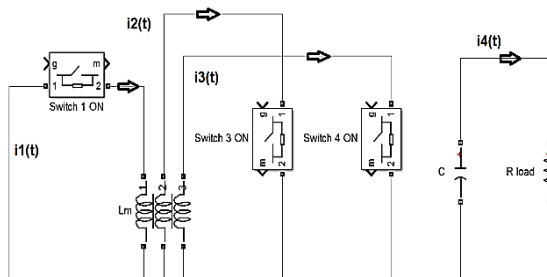


Figure 9: Mode 5 Operation

Mode 6 (t_7-t_8):

In this time interval, the primary inductor L_1 is kept open and mutual fluxes of the inductors, L_2 and L_3 are decreased and induce a mutual current on the coupled inductor pair. The cycle of mode 4-6 is repeated till the operation reaches a time instant of t_9 and modes 1-3 is repeated till it reaches a time instant of t_5 (fig. 10).

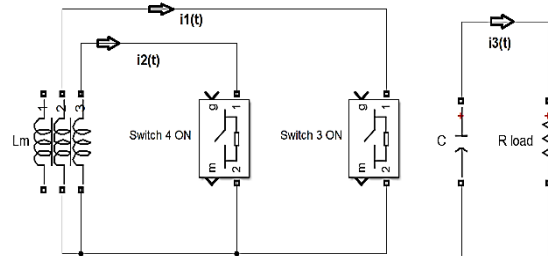


Figure 10: Mode 6 Operation

4. Mathematical Analysis of the Converter

The operation of the circuit can be illustrated in six modes and a number of equations of mutual inductance, current and voltage relation with respect to time is described. The equations are derived from the circuit operating in the six modes.

Mode 1:

$$V_2(t) + R_2 i_4(t) + L_2 \frac{di_4(t)}{dt} + M \frac{d}{dt} (i_3(t) + i_5(t)) = 0 \quad \text{---- (1)}$$

$$V_2(t) + R_3 \cdot i_5(t) + L_3 \frac{di_5(t)}{dt} + M \left(\frac{di_3(t)}{dt} + \frac{di_4(t)}{dt} \right) = 0 \quad \text{---- (2)}$$

$$V_2(t) = \frac{1}{C} \int i_6(t) \cdot dt \quad \text{---- (3)}$$

$$V_2(t) = R_{load} \cdot i_7(t) \quad \text{---- (4)}$$

$$i_3(t) = \frac{V_1(t)}{L_1} e^{\left(\frac{-R_1}{L_1}\right)t} - \frac{M}{L_1} \left[\delta(t) - \left(\frac{R_1}{L_1}\right) e^{\left(\frac{-R_1}{L_1}\right)t} \right] [i_4(t) + i_5(t)] \quad \text{---- (5)}$$

$$i_1(t) = \frac{V_{in} - V_1(t)}{R_{SW2}} \quad \text{---- (6)}$$

$$i_2(t) = \frac{V_1(t)}{R_{SW1}} \quad \text{---- (7)}$$

Mode 2:

$$i_1(t) = \frac{M}{L_1} \left[\delta(t) - \frac{(R_1 + R_{SW1})}{L_1} e^{-\left(\frac{R_1 + R_{SW1}}{L_1}\right)t} \right] [i_2(t) + i_3(t)] \quad \text{---- (8)}$$

$$i_2(t) = -\frac{V(t)}{L_2} e^{-\left(\frac{-R_2}{L_2}\right)t} - \frac{M}{L_2} \left[\delta(t) - \frac{R_2}{L_2} e^{-\left(\frac{-R_2}{L_2}\right)t} \right] [i_1(t) + i_3(t)] \quad \text{---- (9)}$$

$$i_3(t) = -\frac{V(t)}{L_3} e^{-\left(\frac{-R_3}{L_3}\right)t} - \frac{M}{L_3} \left[\delta(t) - \frac{R_3}{L_3} e^{-\left(\frac{-R_3}{L_3}\right)t} \right] [i_1(t) + i_2(t)] \quad \text{---- (10)}$$

$$V(t) = \frac{1}{C} \int i_4(t). dt \quad \text{---- (11)}$$

$$V(t) = R_{load} \cdot i_5(t) \quad \text{---- (12)}$$

Mode 3:

$$i_1(t) = -\frac{V(t)}{L_2} e^{-\left(\frac{-R_2}{L_2}\right)t} - \frac{M}{L_2} \left[\delta(t) - \frac{R_2}{L_2} e^{-\left(\frac{-R_2}{L_2}\right)t} \right] \quad \text{-- (13)}$$

$$V(t) = \frac{1}{C} \int i_3(t). dt \quad \text{-- (14)}$$

$$V(t) = R_{load} \cdot i_4(t) \quad \text{-- (15)}$$

$$i_2(t) = -\frac{V(t)}{L_1} e^{-\left(\frac{-R_1}{L_1}\right)t} - \frac{M}{L_1} \left[\delta(t) - \frac{R_1}{L_1} e^{-\left(\frac{-R_1}{L_1}\right)t} \right] i_1(t) \quad \text{-- (16)}$$

Mode 4:

$$i_1(t) = \frac{V_{in} - V(t)}{R_{SW2}} \quad \text{-- (17)}$$

$$i_2(t) = \frac{V(t)}{R_{SW1}} \quad \text{-- (18)}$$

$$V(t) = R_1 \cdot i_3(t) + L_1 \frac{di_3(t)}{dt} + M \left(\frac{di_4(t)}{dt} + \frac{di_5(t)}{dt} \right) \quad \text{-- (19)}$$

$$i_4(t) = -\frac{M}{L_2} \left[\delta(t) - \frac{(R_{SW3} + R_2)}{L_2} e^{-\left(\frac{R_{SW3} + R_2}{L_2}\right)t} \right] [i_3(t) + i_5(t)] \quad \text{--- (20)}$$

$$i_5(t) = -\frac{M}{L_3} \left[\delta(t) - \frac{(R_{SW4} + R_3)}{L_3} e^{-\left(\frac{R_{SW4} + R_3}{L_3}\right)t} \right] [i_3(t) + i_4(t)] \quad \text{--- (21)}$$

$$R_{load} \cdot i_6(t) - \frac{1}{C} \int i_6(t). dt = 0 \quad \text{--- (22)}$$

Mode 5:

$$i_1(t) = -\frac{M}{L_1} \left[\delta(t) - \frac{(R_{SW1} + R_1)}{L_1} e^{-\left(\frac{R_{SW1} + R_1}{L_1}\right)t} \right] [i_2(t) + i_3(t)] \quad \text{-- (23)}$$

$$i_2(t) = -\frac{M}{L_2} \left[\delta(t) - \frac{(R_{SW3} + R_2)}{L_2} e^{-\left(\frac{R_{SW3} + R_2}{L_2}\right)t} \right] [i_1(t) + i_3(t)] \quad \text{-- (24)}$$

$$i_3(t) = -\frac{M}{L_3} \left[\delta(t) - \frac{(R_{SW4} + R_3)}{L_3} e^{-\left(\frac{R_{SW4} + R_3}{L_3}\right)t} \right] [i_1(t) + i_2(t)] \quad \text{-- (25)}$$

$$R_{load} \cdot i_4(t) - \frac{1}{C} \int i_4(t). dt = 0 \quad \text{-- (26)}$$

Mode 6:

$$(R_2 + R_{SW3})i_1(t) + L_2 \cdot \frac{di_1(t)}{dt} + M \frac{di_2(t)}{dt} = 0 \quad \text{-- (27)}$$

$$(R_3 + R_{SW4})i_2(t) + L_3 \cdot \frac{di_2(t)}{dt} + M \frac{di_1(t)}{dt} = 0 \quad \text{-- (28)}$$

$$R_{load} \cdot i_3(t) - \frac{1}{C} \int i_3(t). dt = 0 \quad \text{-- (29)}$$

4.1 Mutual inductance of the inductor coils

Induced voltage in coil 1

$$V_{L1} = N_1 \frac{d}{dt} (\Phi_{21} + \Phi_{31}) = M \frac{d}{dt} (i_2 + i_3) \quad -- (30)$$

Induced voltage in coil 2

$$V_{L2} = N_2 \frac{d}{dt} (\Phi_{12} + \Phi_{32}) = M \frac{d}{dt} (i_1 + i_3) \quad -- (31)$$

Induced voltage in coil 3

$$V_{L3} = N_3 \frac{d}{dt} (\Phi_{13} + \Phi_{23}) = M \frac{d}{dt} (i_1 + i_2) \quad -- (32)$$

Mutual inductance of inductor L₁:

$$M_1 = N_1 \frac{(\Phi_{21} + \Phi_{31})}{(i_2 + i_3)} \quad -- (33)$$

Mutual inductance of inductor L₂:

$$M_2 = N_2 \frac{(\Phi_{12} + \Phi_{32})}{(i_1 + i_3)} \quad -- (34)$$

Mutual inductance of inductor L₃:

$$M_3 = N_3 \frac{(\Phi_{13} + \Phi_{23})}{(i_1 + i_2)} \quad -- (35)$$

4.2 Total mutual inductance

$$M^3 = M_1 \cdot M_2 \cdot M_3 \quad -- (36)$$

$$M^3 = N_1 \frac{(\Phi_{21} + \Phi_{31})}{(i_2 + i_3)} \cdot N_2 \frac{(\Phi_{12} + \Phi_{32})}{(i_1 + i_3)} \cdot N_3 \frac{(\Phi_{13} + \Phi_{23})}{(i_1 + i_2)} \quad -- (37)$$

$$M^3 = N_1 \cdot N_2 \cdot N_3 \frac{(2k\Phi_1)(2k\Phi_2)(2k\Phi_3)}{(i_1+i_2)(i_2+i_3)(i_1+i_3)} \quad -- (38)$$

$$M = 2kN^3 \sqrt{\frac{\Phi_1 \cdot \Phi_2 \cdot \Phi_3}{(i_1+i_2)(i_2+i_3)(i_1+i_3)}} \quad -- (39)$$

5. Simulation Results of the Model

The phenomenon of switching is accurately done inducing a sinusoidal current in the secondary inductors converting a direct current from the input voltage source to an alternating current of -6.3kA to 3kA through the secondary inductors L₂ and L₃.

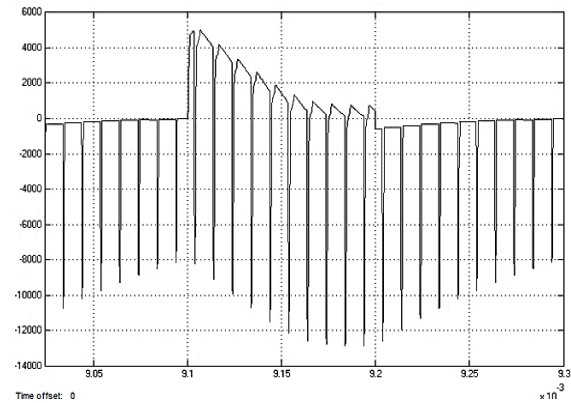


Figure 11: Capacitor Current Curve

Effect of $\frac{dv}{dt}$ can be identified in the primary inductor producing a high voltage of 2250MV which is considered to be unrealistic in practical scenario and can be reduced by implementing an accurate RC snubber circuit. A change in fluctuating current in the secondary inductors creates a continuous change in flux resulting in an induced voltage in the coupled inductors.

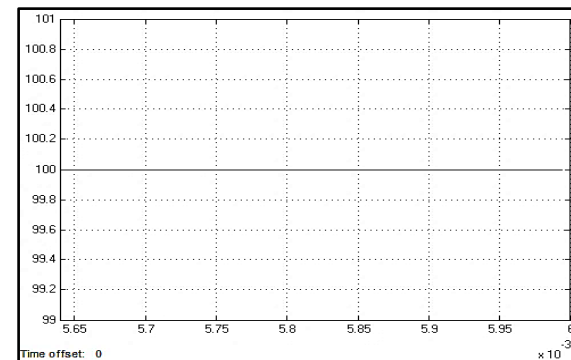


Figure 12: Input Voltage Curve

Capacitor and two identical mutual inductors L₂ and L₃ are acting to be charged and discharged at the same time. A complete time period of SW₃ and SW₄ consisting of two intervals, an interval where the inductors are charged and capacitor is discharged simultaneously and vice-versa. The maximum voltage across the capacitor is 432kV and discharges to a value of 376kV in a cycle. An output voltage of the converter consists of harmonics producing ripples in the output voltage.

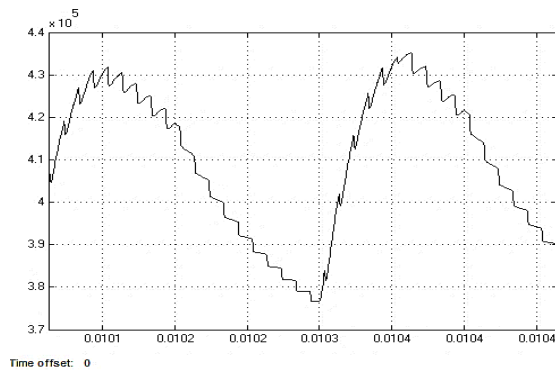


Figure 13: Capacitor Voltage Curve

Load considered in the circuit is resistive of a magnitude of 1kΩ and current flowing through it is 370A to 425A. An effect of harmonics shown in ripples in the output current, resembles to be a periodic signal; whereas the signal should remain constant.

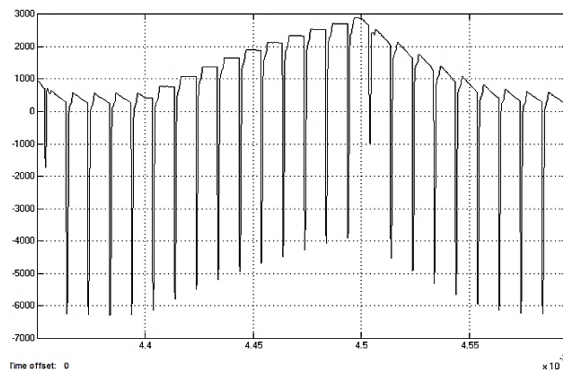


Figure 14: Secondary Inductors Current Curve

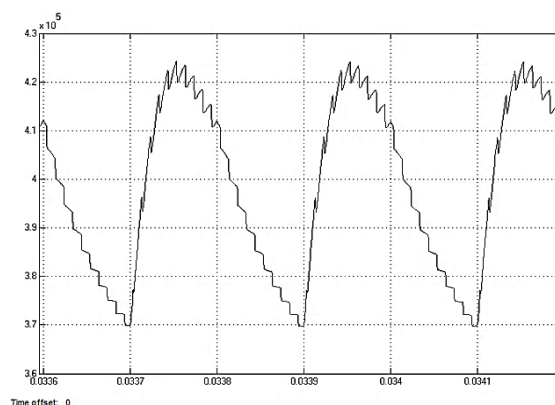


Figure 15: Output Load Voltage Curve

The fundamental component of the circuit is to implement a direct current harmonic filter to reduce the harmonics present in the output waveform which increases the losses in the circuit in the form of heat energy.

Diodes are a component allowing the power to flow unidirectional from inductors to the

capacitor. Current from the capacitor reduces from 5kA to 0A as the capacitor is fully charged within a time period of 0.1ms.

6. Conclusion

In concluding the results of the boost converter, the secondary inductors current starts to increase when the switches SW₃ and SW₄ are turned on and decreases when they are turned off. The load current and voltage are linear for the resistive load, voltage across the load falls when inductors are charged and raised when they turn off as the inductor discharges through the capacitor finally end up charging it. Diodes D₁ and D₂ are forward biased when the switches SW₃ and SW₄ are turned off and reversed biased when they are turned on. Voltages across the secondary inductors are built when the switches are turned off and decreases they are being short circuited by a switching resistance during charging the inductor.

On the other hand, a number of issues are being found in simulating the design in artificial environment. Problem of $\frac{di}{dt}$ is seen in the primary inductors partially reflecting in the secondary inductors and can be reduced by implementing the high $\frac{di}{dt}$ snubber circuit where inductor are connected in specific configuration reducing the sudden increase in current in a short time. A problem of $\frac{dv}{dt}$ is also been found across the inductors and the primary switches and need to be reduced by using the specific configurations of resistance- capacitor snubber circuit.

References

- [1] Y. P. Hsieh, J. F. Chen, T. J. Liang and L. S. Yang, “Novel High Step-Up DC–DC Converter for Distributed Generation System”, *IEEE Transactions on Industrial Electronics*, Vol. 60, Issue No. 4, April 2013, pp. 1473-1482. Doi: doi: 10.1109/TIE.2011.2107721
- [2] O. Cornea, G. D. Andreescu, N. Muntean and D. Hulea, “Bidirectional Power Flow Control in a DC Microgrid Through a Switched-Capacitor Cell Hybrid DC–DC Converter”, *IEEE Transactions on Industrial Electronics*, Vol. 64, Issue No. 4, April 2017, pp. 3012-3022. Doi: 10.1109/TIE.2016.2631527
- [3] D. D. C. Lu, D. K. W. Cheng, and Y. S. Lee, “A Single-Switch Continuous-Conduction-Mode Boost Converter With Reduced Reverse-Recovery and Switching Losses”,

- IEEE Transactions on Industrial Electronics*, Vol. 50, Issue No. 4, August 2003, pp. 767-776. Doi: 10.1109/TIE.2003.814989
- [4] C. Álvarez-Mariño, F. de León, and X. M. López-Fernández, "Equivalent Circuit for the Leakage Inductance of Multiwinding Transformers: Unification of Terminal and Duality Models", *IEEE Transactions on Power Delivery*, Vol. 27, Issue No. 1, January 2012, pp. 353-361. Doi: 10.1109/TPWRD.2011.2173216
- [5] F. de León and J. A. Martinez, "Dual Three-Winding Transformer Equivalent Circuit Matching Leakage Measurements", *IEEE Transactions on Power Delivery*, Vol. 24, Issue No. 1, January 2009, pp. 160-168. Doi: 10.1109/TPWRD.2008.2007012
- [6] Y. C. Hsieh, T. C. Hsueh and H. C. Yen, "A dual-boost converter with zero voltage transition", *2008 IEEE Power Electronics Specialists Conference*, Rhodes, 2008, pp. 692-696. Doi: 10.1109/PESC.2008.4592010
- [7] M. Veerachary and J. Prakash, "Zero-voltage switching of high-gain boost converter", *2016 IEEE 1st International Conference on Power Electronics, Intelligent Control and Energy Systems (ICPEICES)*, Delhi, 2016, pp. 1-6. Doi: 10.1109/ICPEICES.2016.7853674
- [8] M. H. Rashid (Ed.), *Power Electronics Handbook: Devices, Circuits and Applications*, Third Edition, pp. 249, Elsevier, MA, USA, 2011.
- [9] C. W. T. McLyman, *Transformer and Inductor Design Handbook, 4th Edition*, CRC Press, 2011.
- [10] A. Chakraborty, *Circuit theory Analysis and Synthesis*, Sixth Revised Edition, pp. 455, Dhanpat Rai & Co. Pvt. Ltd, New Delhi, 2006.
- [11] S. Chowdhury, S. P. Chowdhury and P. Crossley, *Microgrids and Active Distribution Networks*, The Institution of Engineering and Technology, 2009. Doi: <http://dx.doi.org/10.1049/PBRN006E>
- [12] N. Jenkins, G. Strbac and J. Ekanayake, *Distributed Generation*, The Institution of Engineering and Technology, 2010. Doi: <http://dx.doi.org/10.1049/PBRN001E>
- [13] S. Jain, *Modeling and Simulation Using MATLAB-Simulink*, 2nd Edition, pp. 429, Wiley India Publication, New Delhi, 2015, ISBN: 9788126551972.